IMPROVEMENT OF HOT CORROSION RESISTANCE OF AUSTENITIC STAINLESS STEEL 316L IN ASH BY CHROMIZING-SILICONIZING

Dr. Ali Hobi Halem   **Dr. Hayder Hassan Jaber**   **Roaa Hatim Hatif**
alialihhhobi@yahoo.com

ABSTRACT

The simultaneous deposition of Cr and Si into austenitic stainless steel 316L alloy using a halide-activated pack-cementation process is described, using a pack mixture containing (67 wt. % Cr, 8 wt. % Si, 2 wt. % NH_4Cl, 23 wt. % Al_2O_3). The diffusion coating process is carried out at 950^oC for 6hrs under Ar atmosphere. It was found that diffusion coating time produce coating thickness of 80-100µm, the corrosion resistant properties of austenitic stainless steel can be improved by enriching the surface composition in Cr and Si using pack cementation process, this study compare the hot corrosion performance of uncoated and coated austenitic stainless steel 316L with chromized-siliconized diffusion coating specimens in the presence of molten mixture of Na_2So_4 and V_2O_5 at 850^oC and compare the micro-hardness between them. In the case of coated austenitic stainless steel 316L alloy with chromized-siliconized diffusion coating, specific weight gain will be observed while specific weight lose can be observed in the case of uncoated austenitic stainless steel 316L alloy. Diffusion coated austenitic stainless steel 316L alloy has shown excellent corrosion resistance and higher micro hardness than uncoated austenitic stainless steel 316L alloy because the coated layer that consisted mainly of $CrSi_2$ and Cr_3

Keywords: diffusion coating, pack cementation, hot corrosion, stainless steel 316L, ash.

الخلاصه:

تشيرنتائج الدراسةالحالية إلى إمكانية زيادة مقاومة التأكل الحار للفولاذ المقاوم للصدأ الأوستنايتي (Austenitic AISI stainless steel 316L) منخلا لزيادة محتوىا لكروم و السليكون عن سطح الفولاذ باستخدام تقنية الطلاء الانتشاري بالسمنتة (Pack Cementation). تم إجراء ترسيباً آنيا بالكروم والسليكون على سبيكة الفولاذ المقاوم للصدأ الاوستينايتي 316 L باعتماد ألية الطلاء الانتشاري، وذلك باستخدام خليط مكون من: (67% Cr،8Si% ، NH_4Cl%2 ، Al_2O_3%23). جرت عملية الطلاء ألانتشاري عند درجة حرارة 950 مُ ولمدة (6 ساعات) فيجومنالآركون . ولقدوجدإنسمكطبقة حوالي (80- 100 مايكرومتر)،يمكن تحسين مقاومة التآكل للفولاذ الأوستنايتي من خلال زيادة محتوى الكروم والسليكون على السطح، تقوم هذه الدراسة باجراء مقارنة بين الفولاذالاوستنايتيL316الغير مطلي والمطلي بطبقة من الكروم وبوجودخليطمنالمنصهر الملحي Na_2So_4 وV_2O_5عند درجة حراره 850 مْوكذلك مقارنة قيم الصلادة بين طبقة الطلاء والمعدن الأساس. ففي حالة الفولاذ الغير مطلي نلاحظ فقدان بالوزن النوعي للفولاذ الاوستنايتي بينما نلاحظ زياده ملحوظه بالوزن النوعي عندما يكون الفولاذ مطليا بطبقه من الكروم والسليكون وكذلك نلاحظ زيادة قيم الصلادة بالنسبة لطبقة الطلاء أكثر من المعدن الأساس وذلك يعود الي التركيب الطوري حيث تتكون طبقة الطلاء بشكل رئيسي من $CrSi_2$وCr_3Si.

ففي حالة الفولاذ الغير مطلي نلاحظ فقدان بالوزن النوعي للفولاذ الاوستنايتي بينما نلاحظ زياده ملحوظة بالوزن النوعي عندما يكون الفولاذ مطليا بطبقه من الكروم والسليكون وكذلك نلاحظ زيادة قيم الصلادة بالنسبة لطبقة الطلاء أكثر من المعدن الأساس وذلك يعود إلي التركيب ألطوري حيث تتكون طبقة الطلاء بشكل رئيسي من $Cr\ Si_2$ و Cr_3Si.

1. INTRODUCTION

The performance of different alloys exposed to high temperature depends upon their mechanical resistance as well as their corrosion / oxidation properties. When the mechanical requirements are not critical, austenitic stainless steels may play a role in substituting the more expensive Ni and Co based alloy (Kushan, 2012). Materials such as vanadium pentoxide (V_2O_5), and sodium sulfate (Na_2SO_4) is the most corrosive at elevated temperatures (Habibi, 2013), sodium sulfate along with the vanadates (V_2O_5, etc.) can then form molten deposits on the surface of gas turbine airfoils. This molten salt mixture in the presence of a partial pressure of SO_2/SO_3 provided by the combustion gases generates a fluxing (dissolving) of the protective oxide scale and inhibits its reformation. If allowed to progress unchecked, catastrophic attack of the underlying substrate metal will result.   Stainless steels have served as the workhouse material in the construction of power generation installations. However, these steels suffer from corrosion attack in the forms of oxidation, sulfidation, and deposition corrosion in these applications. In particular, sulphidation, resulting from the presence of sulfur in low grade fuel, shortens the service life of these structures considerably (Zhang, 2011).Appropriate coatings, applied to stainless steels, have long been sought as a means to combat these corrosion problems. Physical vapor deposition (PVD), chemical vapour deposition (CVD), thermal spray and plasma spray have various advantages and disadvantages(Parsapour, 2005). The associated high costs for low pressure vapour deposition equipment limits its acceptability for large scale applications. Spraying methods make impractical to protect certain geometries such as these inside walls of heat exchangers tubing. Also, some spray coatings suffer oxidation, high porosity and poor adhesion to the substrate material, leaving them particularly vulnerable to corrosion attack (Kushan, 2012).

2. EXPERIMENTAL DETAILS

a. Material

The substrate alloy used in this steady was austenitic stainless steels 316L. The sepectrochemical analysis was carried out at General Company for examination and rehabilitation engineering/ Baghdad, as shown in (Table 1). Austenitic stainless steels specimens were cut into circular shapes as shown in (Fig. 1), the dimensions of specimens were 20mm in diameter and 4mm in thickness with total surface area $8.8 \times 10^4\ mm^2$. First all surfaces of these specimens were grinding using 120, 220, 320, 600, 800, and 1200 grit silicon carbide papers. These specimens were then cleaned with water and then ultrasonically cleaned for 30 minutes using ethanol as a medium. The coated and uncoated specimens of austenitic stainless steel 316L alloy were studied in (67 wt. %V_2O_5/33+wt. %Na_2SO_4) at 550°C, 650°C, 750°C, 850°C, 950°C for 4hrs.

b. Processing

Austenitic stainless steel 316L alloy specimen was placed in a sealed carbon steel cylindrical retort of 50mm in diameter and 80mm in height in contact with the pack mixture. The retort was then put in another stainless steel cylindrical retort of 80 mm in a diameter and 140mm in height. The outer retort has a side tube through which argon gas passes and second in the top cover for argon gas outlet. This combined system is put in an electrical holding furnace under an argon atmosphere with a flow rate of 1.5 L/min to avoid the oxidation of the underlying materials during the process. (Fig.2) shows schematic diagram of pack cementation apparatus. The simultaneous chromizinorg-siliconizing treatments were conducted at $950^{o}C$ 6hrs as shown in (Fig. 3), after coating, the packs were cooled to room temperature in the same furnace, and the specimens were ultrasonically cleaned to remove only loosely entrapped pack material on the surface.

c. Characterization

The cross sections of each specimen were cut using low speed saw and polished for examination using optical microscopy, microhardness, scanning electron microscopy (SEM). After and before coating, X-ray diffraction (XRD) was used to determine the phase structures at the surface layer of the as received uncoated austenitic stainless steel 316L alloy; this test shows that only three main peaks are present in the limited scope of 2θ from 10 to 90 degrees. These three peaks are related to chromium iron nickel (Cr-Fe-Ni) austenitic steel as shown in (Fig. 4). (Fig. 5) shows the phases that formed in the surface layer of coated austenitic stainless steel 316L alloy with chromized-siliconized diffusion coating which consist mainly of $CrSi_2$ and Cr_3Si. During pack cementation chromium and silicon diffuses into the substrate and results in a phase transformation. (Fig.6) shows the typical morphology by SEM of coated austenitic stainless steel 316L alloy with chromized-siliconized diffusion coating coated in the pack powder mixture. (Fig. 7) shows EDX pattern of the concentration variations of Cr and Si near the surface to the uncoated and coated specimen respectively. To investigate hot corrosion characteristics, The specimens were measured and weighed first, then deposited 5mg/cm^2 from ash mixture and placed in furnace at different heating intervals for various temperatures (550, 650, 750, 850 and $950^{o}C$) for 4hrs at each temperature according to Alsultani procedure (Alsultani, 2003). After testing the specimens were cleaned in an ultrasonic bath, first in distilled water and then in ethanol. They were then weighed to determine the change in weight.

3. RESULTS AND DISCUSSION

a. Hot Corrosion Results

An initial lose in measured weight was observed in austenitic stainless steel 316L alloy after subjection to vanadic slag mixture (67 wt. %V_2O_5 +33 wt. % Na_2SO_4) at (550, 650, 750, 850 and $950^{o}C$) for 4hrs at each temperature as shown in (Fig. 8).General conclusion from this figure show that the increase in temperature leads to increase in specific weight loss and hence vanadic slag accelerated oxidation of uncoated austenitic stainless steel 316L alloy.
In the temperature range of $900^{o}C$, the Na_2SO_4 and V_2O_5 will combine to form $NaVO_3$, as represented by (Eq. 1) having a melting point of $610^{o}C$ (Smeltzer, 1975) [106]:

$$Na_2SO_4 + V_2O_5 \longrightarrow 2NaVO_{3\,(l)} + SO_2 + (1/2)\,O_2 \qquad (1)$$

The introducing of sodium vanadates $NaVO_3$ is an indication of the role of molten sodium vanadate on introducing oxygen to react with the iron surface so that it catalysed the oxidation of the metal (Gurrappa, 1999). This is a known behavior of vanadium compounds in

oxidation processes. Furthermore, the in situe formed oxide dissolves in the molten layer of the ash compounds. Thus, the molten ash is the major cause of the oxidation of iron and its gradual depletion, so that the continued heating results in continuous consumption of the metal.

The effect of ash on the steel surface confirmed the oxidation and dissolution of (Fe_2O_3) in the molten scale in addition to the format of several types of sodium vanadates. (Fig. 9) shows that the formation of surface attack in which void-layers with different void densities is formed layer by layer. The phases of scale formed on uncoated austenitic stainless steel 316L alloy in the presence of (67 wt. %V_2O_5 +33 wt. % Na_2SO_4) was examined in XRD analysis. (Fig. 10) illustrate the major phases exist on uncoated stainless steel 316L alloy surfaces at oxidizing with 67 wt. %V_2O_5 +33 wt. % Na_2SO_4 which are Cr_2O_3, Ni-Cr-Fe and NiO. For coated austenitic stainless steel 316L alloy with chromized-siliconized diffusion coating after deposited in (67 wt. % V_2O_5 + 33 wt. % Na_2SO_4) is shown in (Fig. 11), the coated austenitic stainless steel 316L alloy showed much lesser overall weight gain as compared to uncoated specimens in the given molten salt environment. The formation of phases like Cr_2O_3 and SiO_2 in the protective scale of the coatings was suggested to induce requisite resistance in the steels.(Fig. 12) shows LOM images of coated austenitic stainless steel 316L alloy with chromized-siliconozed diffusion coating after cyclic oxidation in deposited salt (67 wt. %V_2O_5 +33 wt. % Na_2SO_4) at different heating intervals for various temperature (550, 650, 750, 850 and 950°C) for 4hrs at each temperature.(Fig. 13) illustrate the major phases exist on coated austenitic stainless steel 316L alloy with chromized-siliconozed diffusion coating surfaces after cyclic oxidation in the presence of (67 wt. %V_2O_5 +33 wt. % Na_2SO_4) which are SiO_2,Cr_3Si and Cr_2O_3.

b. Micro-Hardness Results

For practical application, the influence of the coating layer on the hardness value of the substrate alloy must also be concerned. Resulted from microhardness of the substrate alloy and coated layer are given in (Table 2).The hardness of the coated austenitic stainless steel 316L alloy with chromized-siliconozed diffusion coating is higher than the austenitic stainless steel 316L alloy substrate. This increase of hardness is apparently due to the hard and brittle phases exist at the surface $CrSi_2$ and Cr_3Si.

4. CONCLUSION

For coated austenitic stainless steel 316L alloy with chromized-siliconized diffusion coating revealed good cyclic oxidation resistance compared With uncoated austenitic stainless steel 316 L alloy for 52 hrs at 4hrs cycle at 850 C Can be described , specific weight loss can be noted for uncoated austenitic stainless steel 316 L alloy oxides With   (67 wt. % V_2O_5 + 33 wt. % Na_2SO_4) . While specific Weight gain can be noted for coated austenitic stainless steel 316 L alloy With chromized-siliconozed diffusion coating after cycli oxidation in deposited salt (67 wt. % V_2O_5 + 33 wt. % Na_2SO_4) . Vicker's microhardness tests reveal that the hardness of the coated layer is higher than that for the austenitic stainless steel 316 L alloy substrate , under the same conditions .

Table (1): Spectrochemical analysis of austenitic stainless steel in wt. %.

EL	Fe	C	Mn	Si	Cr	Ni	P	S	Mo	V	Cu
Wt.%	bal.	0.041	1.42	0.27	19.38	10.24	0.025	0.003	0.283	0.080	0.218

Table (2): Overview of Vicker's hardness number for 316L alloy with chromizing-siliconizing diffusion coating.

Location	Vicker's hardness number
Coated layer	1200 HV
316L substrate	492 HV

Figure (1): Austenitic stainless steel 316L alloy (a) as polished, and (b) as coated condition (chromizied-siliconized diffusion coating specimen).
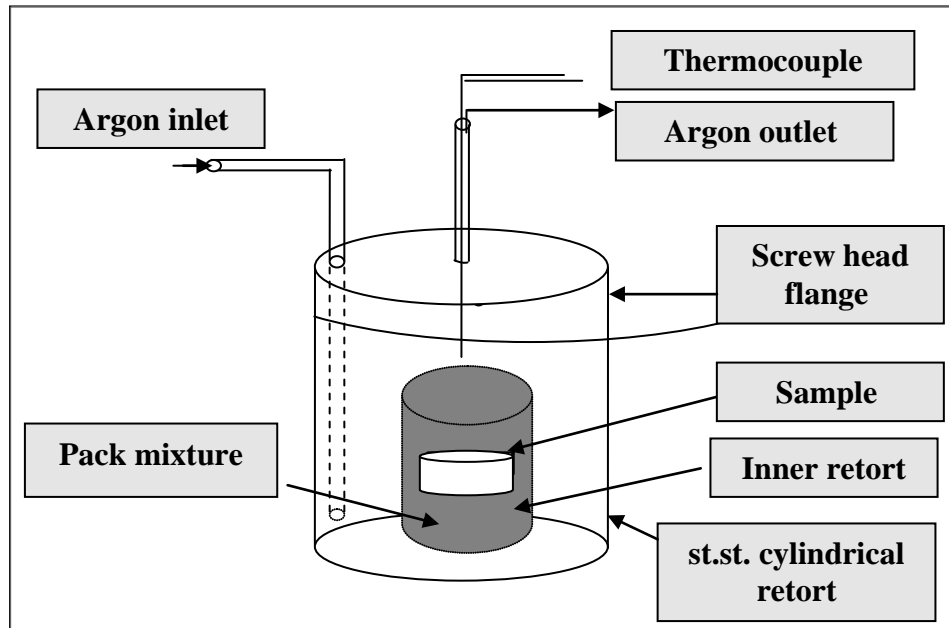
Figure (2): Schematic diagram of pack cementation apparatus.
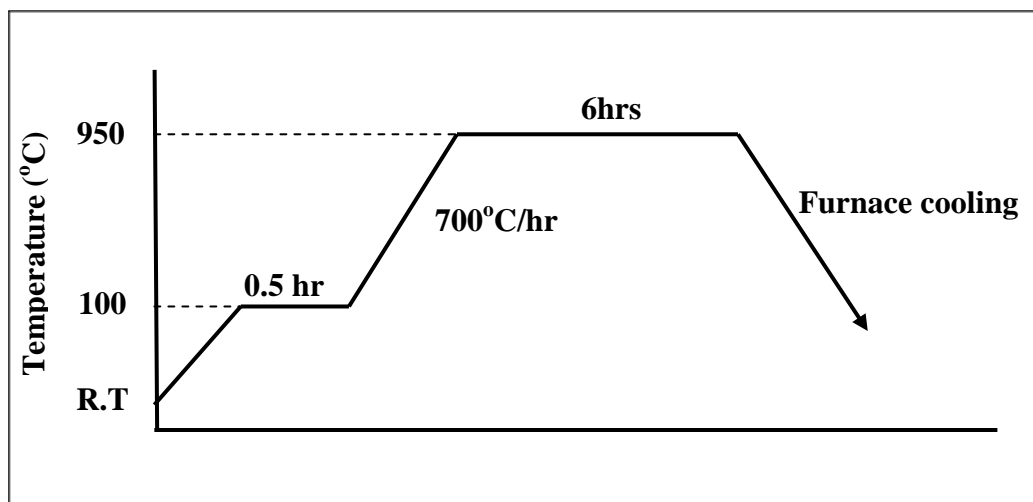
Figure (3): Heating cycle for one step pack cementation process.
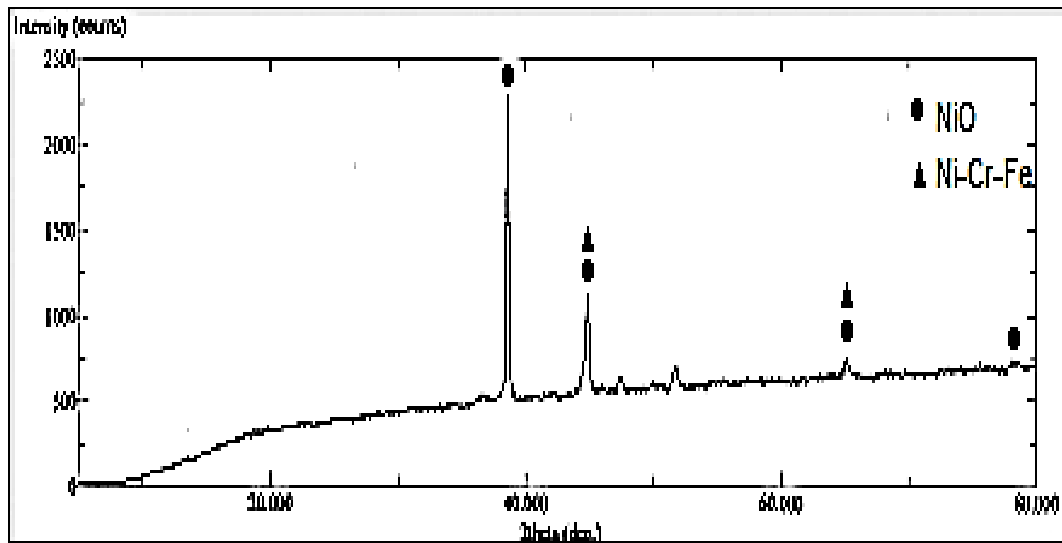
Figure (4): Diffractograms from the surface of uncoated austenitic stainless steel 316L alloy.
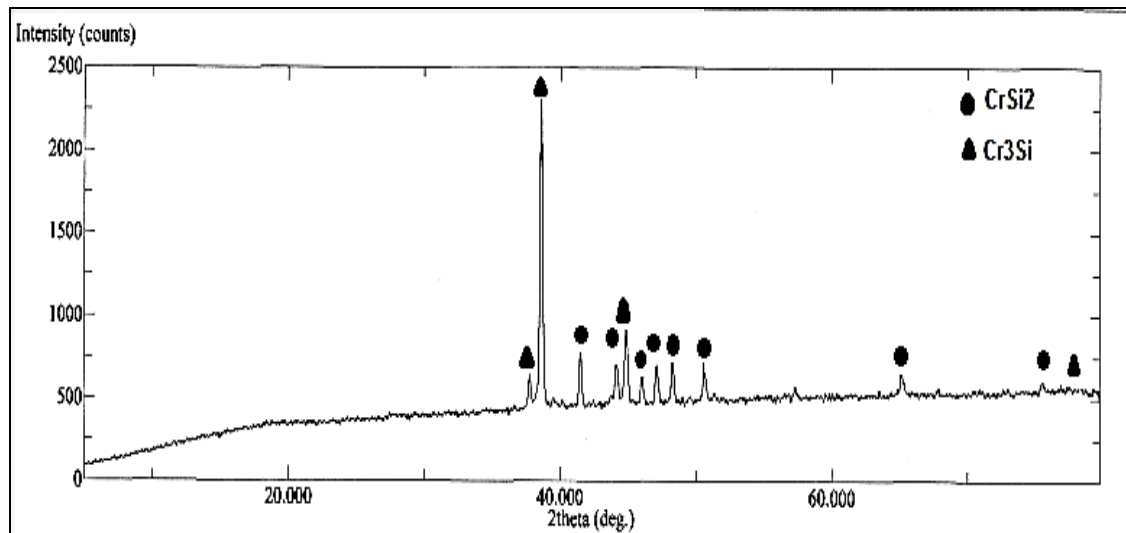
Figure (5): Diffractograms from the surface of coated austenitic stainless steel 316L alloy with chromized-siliconized diffusion coating.
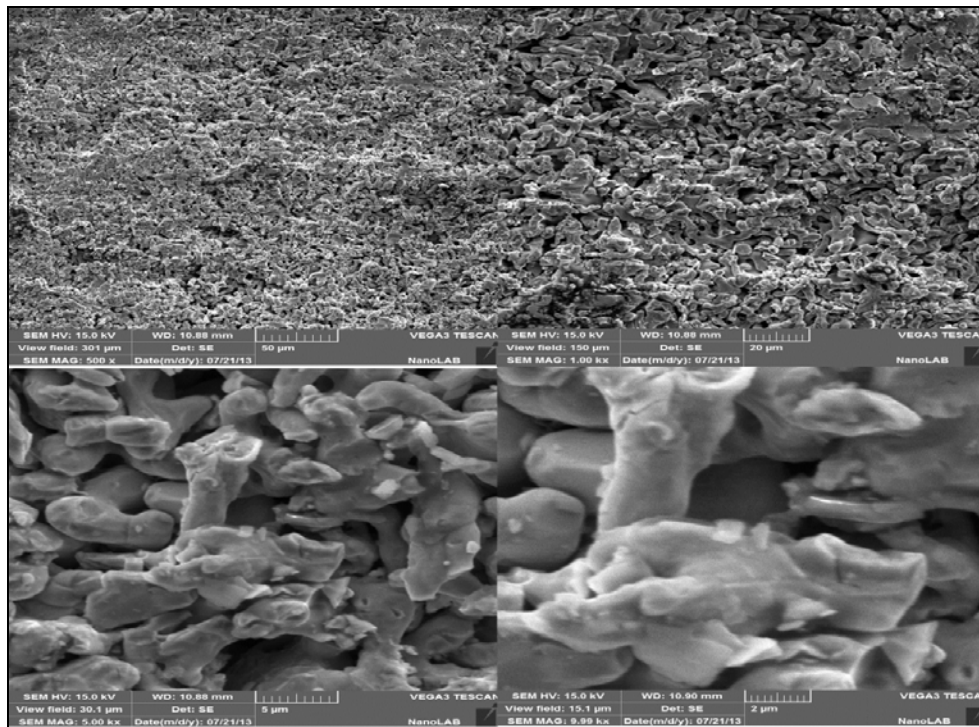
**Figure (6): SEM image of coated austenitic stainless steel 316L alloy
with chromized-siliconized diffusion coating.**

**IMPROVEMENT OF HOT CORROSION RESISTANCE
OF AUSTENITIC STAINLESS STEEL 316L IN ASH BY
CHROMIZING-SILICONIZING**

**Dr. Ali H. Halem
Dr. Hayder H. Jaber
Roaa H. Hatif**
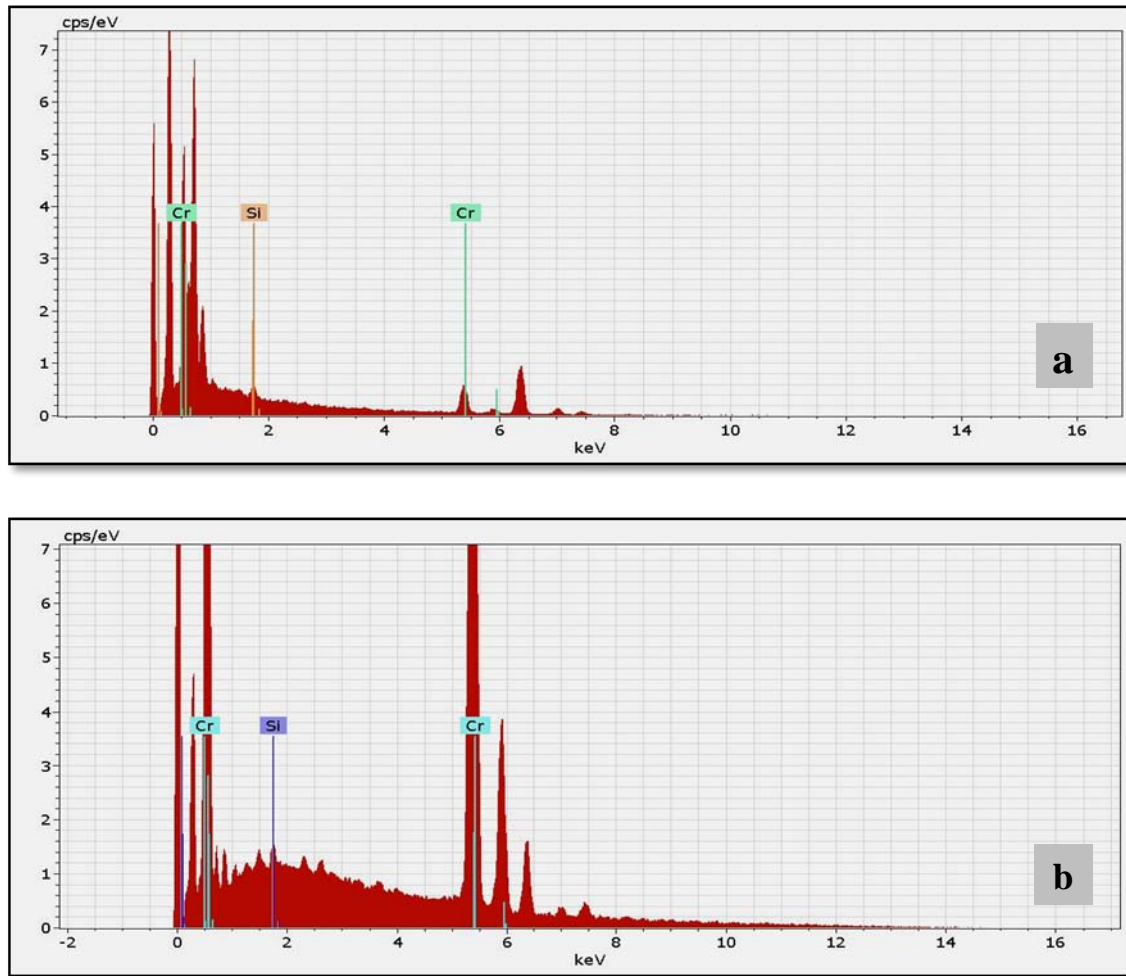
Figure (7): EDX pattern showing the concentration variations of Cr and Si near the surface at 950ºC for 6hrs (a) uncoated, (b) coated specimen.
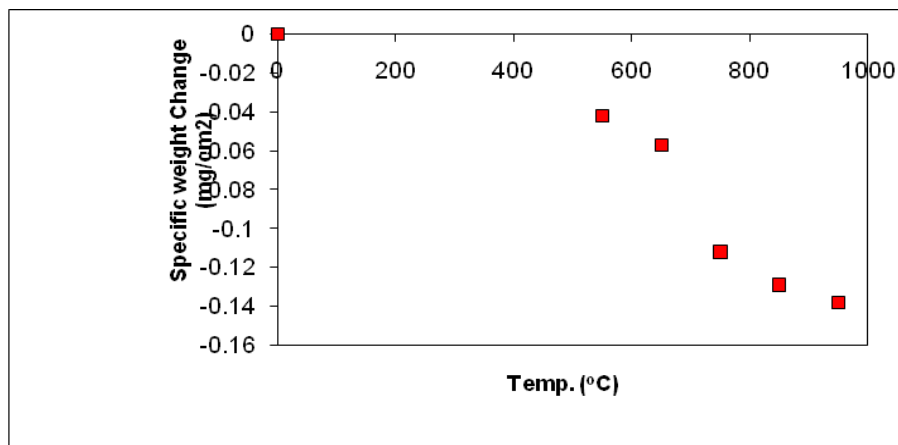
Figure (8): The relation between specific weight change and different heating intervals for uncoated austenitic stainless steel 316L alloy for various temperatures (550, 650, 750, 850 and 950ºC) for 4hrs at each temperature.
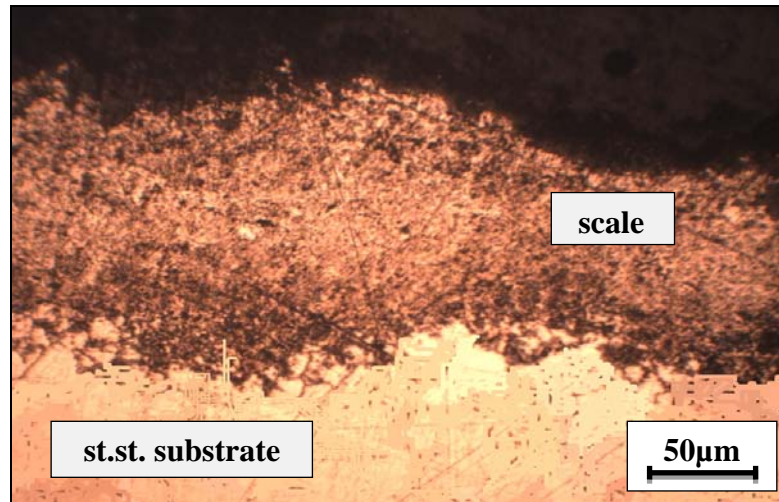
Figure (9): Cross section image of LOM of uncoated austenitic stainless steel 316L alloy oxidized with (67 wt. %V_2O_5 +33 wt. % Na_2SO_4).
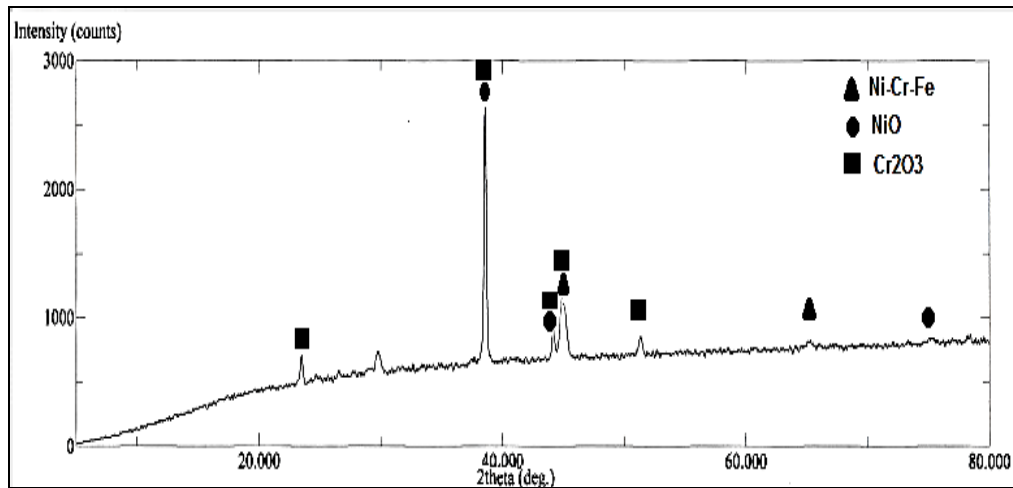
Figure (10): Diffractograms from the surface of uncoated austenitic stainless steel 316L alloy oxidized with (67%V_2O_5+33%Na_2SO_4).
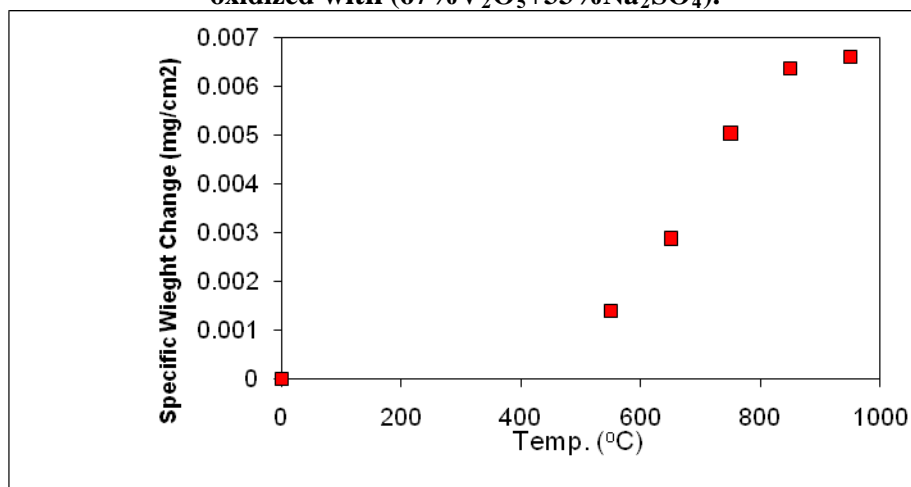
Figure (11): The relation between specific weight gain and different heating intervals of coated austenitic stainless steel 316L alloy with chromized-siliconozed diffusion coating.

IMPROVEMENT OF HOT CORROSION RESISTANCE
OF AUSTENITIC STAINLESS STEEL 316L IN ASH BY
CHROMIZING-SILICONIZING

Dr. Ali H. Halem
Dr. Hayder H. Jaber
Roaa H. Hatif
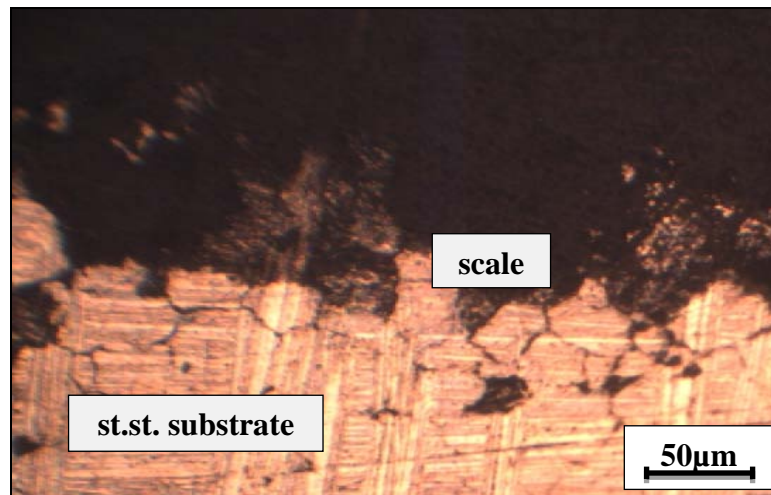
Figure (12): Cross section image of LOM of coated austenitic stainless steel 316L alloy with chromized-siliconozed diffusion coating after cyclic oxidation in deposited salt (67 wt. %V$_2$O$_5$ +33 wt. % Na$_2$SO$_4$).
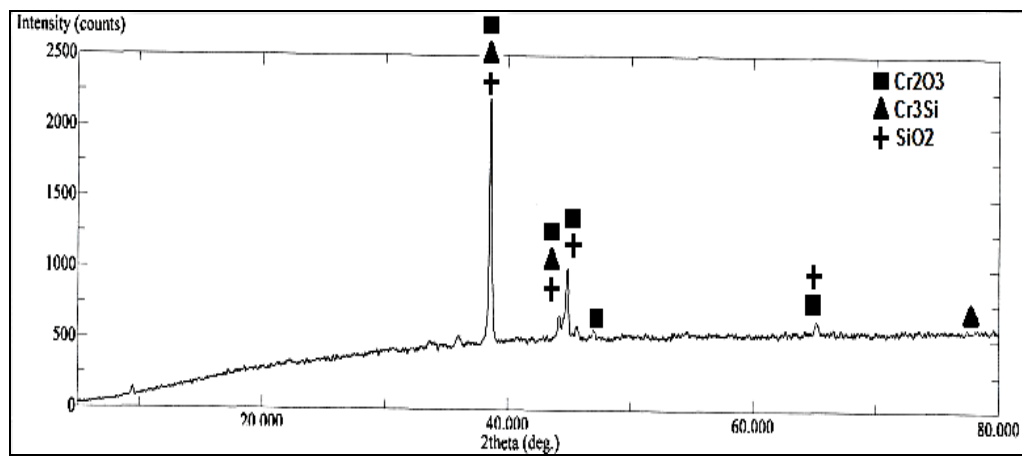
Figure (13): Diffractograms from the surface coated austenitic stainless steel 316L alloy with chromized-siliconozed diffusion coating after cyclic oxidation in deposited salt (67 wt. %V$_2$O$_5$ +33 wt. % Na$_2$SO$_4$).

5. REFERENCES

A. Parsapour, M. H. Fathi and M. Salehi, (2005), "In Vitro Evaluation of the Corrosion Behavior and Biocompatibility of Surface Treated and Metallic Coated Stainless steel 316L Important", Proceeding of the First Jordan International Conference of Materials Science and Engin eering, Al-Salt, pp. 91-99, (2005).

I. Gurrappa, (1999), "Hot Corrosion Behavior of CM247LC Alloy in Na_2SO_4 and NaCl Environments", Oxidation of Metals, Vol.51, Nos.5/6, pp.123-143, (1999).

K. F. Alsultani, (2003), "A Pilot System for Evaluation of Hot Ash Corrosion Inhibition in Power Generation System",PhD. Thesis, the Chemical Eng. Department, the Technology University, Iraq, (2003).

K. Zhang, M. M. Liu, S. L. Liu, C. Sun and F. H. Wang, (2011), "Hot Corrosion Behaviour of A Cobalt-Base Super-Alloy K40S with and without Nicralysi Coating", Corrosion Science Vol. 53,pp. 1990–1998, (2011).

M. C. Kushan, S. C. Uzgur, Y. Uzunonat, and F. Diltemiz, (2012), "ALLVAC 718 Plus™ Superalloy for Aircraft Engine Applications",pp. 75-96, (2012).

M. H. Habibi, L. Wang, J. Liang and S. M. Guo, (2013), "An Investigation On Hot Corrosion Behavior Of YSZ-Ta_2O_5 In Na_2SO_4+V_2O_5 Salt At 1100^oC", Corrosion Science,Vol. 75, pp.409–414, (2013).

W. W. Smeltzer and D. S. Young, (1975), "Oxidation Properties of Transition Metals", Progress in Solid State Chemistry, Vol.10, part1, pp.17-54, (1975).